



香港城市大學
City University of Hong Kong

專業 創新 胸懷全球
Professional · Creative
For The World

CityU Scholars

Potential Power Output from Vehicle Suspension Energy Harvesting Given Bumpy and Random-Surfaced Roads

Guo, Hengyu; Zeng, Weijun; Egloff, Dario; Meng, Fei; Dahlsten, Oscar

Published in:
Sustainability (Switzerland)

Published: 01/08/2024

Document Version:
Final Published version, also known as Publisher's PDF, Publisher's Final version or Version of Record

License:
CC BY

Publication record in CityU Scholars:
[Go to record](#)

Published version (DOI):
[10.3390/su16166964](https://doi.org/10.3390/su16166964)

Publication details:
Guo, H., Zeng, W., Egloff, D., Meng, F., & Dahlsten, O. (2024). Potential Power Output from Vehicle Suspension Energy Harvesting Given Bumpy and Random-Surfaced Roads. *Sustainability (Switzerland)*, 16(16), Article 6964. <https://doi.org/10.3390/su16166964>

Citing this paper

Please note that where the full-text provided on CityU Scholars is the Post-print version (also known as Accepted Author Manuscript, Peer-reviewed or Author Final version), it may differ from the Final Published version. When citing, ensure that you check and use the publisher's definitive version for pagination and other details.

General rights

Copyright for the publications made accessible via the CityU Scholars portal is retained by the author(s) and/or other copyright owners and it is a condition of accessing these publications that users recognise and abide by the legal requirements associated with these rights. Users may not further distribute the material or use it for any profit-making activity or commercial gain.

Publisher permission

Permission for previously published items are in accordance with publisher's copyright policies sourced from the SHERPA RoMEO database. Links to full text versions (either Published or Post-print) are only available if corresponding publishers allow open access.

Take down policy

Contact lbscholars@cityu.edu.hk if you believe that this document breaches copyright and provide us with details. We will remove access to the work immediately and investigate your claim.

Article

Potential Power Output from Vehicle Suspension Energy Harvesting Given Bumpy and Random-Surfaced Roads

Hengyu Guo ^{1,2} , Weijun Zeng ^{3,4} , Dario Egloff ⁵ , Fei Meng ⁶  and Oscar Dahlsten ^{6,2,*} 

- ¹ Department of Computer Science, The University of Hong Kong, Hong Kong SAR, China; guohy@connect.hku.hk
- ² Department of Physics, Shenzhen Institute for Quantum Science and Engineering, Southern University of Science and Technology, Xueyuan Boulevard, Nanshan District, Shenzhen 518055, China
- ³ School of Innovation and Entrepreneurship, Southern University of Science and Technology, Xueyuan Boulevard, Nanshan District, Shenzhen 518055, China; weijun.zeng@aalto.fi
- ⁴ Low Temperature Laboratory, Department of Applied Physics, Aalto University School of Science, P.O. Box 15100, 00076 Aalto, Finland
- ⁵ Departamento de Física, Universidad de los Andes, Carrera 1 # 18A-12, Bogotá 111711, Colombia; d.egloff@uniandes.edu.co
- ⁶ Department of Physics, City University of Hong Kong, Tat Chee Avenue, Kowloon, Hong Kong SAR, China; fmeng@cityu.edu.hk
- * Correspondence: oscar.dahlsten@cityu.edu.hk

Abstract: The energy efficiency of vehicles is a crucial challenge relating to sustainable energy preservation and regeneration methods. Regenerative braking has proven feasible, and there is interest in whether harvesting energy from a vehicle's suspension is similarly feasible. We here provide methods for estimating the amount of power that can be regenerated from the suspension for given vehicle and road parameters. We show that a reasonable road model is a generalised Gaussian process known as AR(1). Using this model, we can derive the key equation used in the ISO 8608 standard for measuring road roughness, such that the AR(1) parameters can be related to the measured road roughness data. We find that the road roughness coefficient of ISO 8608 and the diffusion coefficient of the AR(1) road are equal up to a factor. We provide an analytical expression for the maximum amount of power that can be generated for given road and car parameters, derived via Fourier analysis. We further model harvesting from large bumps using Simulink. These results help to estimate the potential power output given the measured road data.

Keywords: regenerative vehicle suspension energy harvesting; AR(1) Gaussian road; quarter car



Citation: Guo, H.; Zeng, W.; Egloff, D.; Meng, F.; Dahlsten, O. Potential Power Output from Vehicle Suspension Energy Harvesting Given Bumpy and Random-Surfaced Roads. *Sustainability* **2024**, *16*, 6964. <https://doi.org/10.3390/su16166964>

Academic Editor: Jack Barkenbus

Received: 25 June 2024

Revised: 19 July 2024

Accepted: 6 August 2024

Published: 14 August 2024



Copyright: © 2024 by the authors. Licensee MDPI, Basel, Switzerland. This article is an open access article distributed under the terms and conditions of the Creative Commons Attribution (CC BY) license (<https://creativecommons.org/licenses/by/4.0/>).

1. Introduction

Energy harvesting has been a central concern in human technology historically and continues to be so today. This includes the practice of harvesting energy from motion [1,2]. A basic principle of energy harvesting from motion created by humans, such as our body motion or vehicle motion, is to harvest energy that is otherwise lost as friction [2] so that one gains energy without impeding the desired motion. A potential source for such energy is the undesired vertical motion of vehicle bodies, which is presently typically lost as heat in the suspension system.

There is accordingly significant research into harvesting energy from suspension systems (see Refs. [3–5] for reviews). There are proposals involving variable damping coefficients [6], active suspension [7,8], regenerative control [9], and more [5,10–12]. There are several companies undertaking research on suspension harvesting (see, for example, Refs. [13,14]).

A crucial question in such research is how much energy can be extracted. The rough amount of energy available in passenger cars is estimated at 100–400 W [15,16]. The amount of energy that can potentially be recovered from the suspension depends on both the car

and the road parameters. Understanding this dependence is important for judging the feasibility of suspension harvesting and what the optimal power outputs are.

In this article, we provide several results concerning the possible power output from the suspension as a function of the road and vehicle parameters. We employ numerical and analytical tools, including stochastic processes models and system dynamics methods [17]. We employ the widely used quarter car model which is regarded as accurate while not being too complex [18,19]. In the quarter car model, one models a quarter of the car, as illustrated in Figure 1. We model the road either as having randomly distributed uneven bumps or speed bumps. The model we propose using for randomly distributed bumps is known as the AR(1) process (autoregressive model of order 1) [20]. In this process, there are random changes in the vertical profile of the surface, as well as a degree of memory of the surface at the previous point. We show that this model matches the ISO 8608 standard [21] for road roughness well. We find that the road roughness coefficient of ISO 8608 and the diffusion coefficient of the AR(1) road are equal up to a factor. We model replacing the resistive dampening in the suspension with an energy harvester. This approach is chosen so that the energy harvesting does not impact the motion differently to a normal suspension. We consider both resistive loads and supercapacitor loads. We provide numerical simulations and analytical expressions concerning how much power can be extracted for the given road and vehicle parameters.

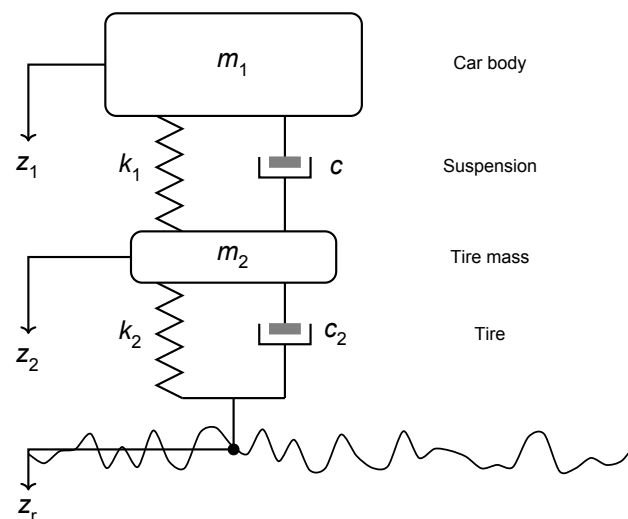


Figure 1. Typical quarter car model (see, for example, Ref. [17]). The first block in this picture represents one quarter of the car body which has mass m_1 . The spring with the spring constant k_1 and the damper with the damping coefficient $c_1 := c$ form the suspension system. The lower mass m_2 and the associated damper and spring represent the wheel. We analyse replacing the damper c between the two bodies with an energy harvester. The power is harvested from the relative motion $\dot{z}_{\text{rel}} = \frac{d}{dt}(z_1 - z_2)$. The road height z_r is modelled as either being generated by a stochastic process called AR(1) or as having a speed bump.

2. One Speed Bump

This section concerns how much power can be extracted from a single speed bump. We firstly describe the simulation model and then analyse how much power can be harvested when the car goes over the bump.

2.1. Simulation Model

We model a speed bump by generating a road height $z_r(t) = H \sin(\frac{\pi v}{L} t)$, where H is the maximal height, L is the length, v is the car speed, and t is the time. The bump is depicted in Figure 2. We use this model because it is stated to be a good approximation for the commonly used circular speed bump [22,23].

In the simulation, the harvester replaces the damper c shown in Figure 1. We employ the paradigm that only energy otherwise dissipated as heat may be harvested, such that the motion of the vehicle is not altered relative to the normal suspension when the harvester is introduced. Whilst in some circumstances, such as water wave energy harvesting [24], it can be advantageous to optimise power output by maximising the motion, in the case of vehicle suspension, this is clearly not desired. The damping force from the harvester is modelled as $F_{\text{damp}} = -c\dot{z}_{\text{rel}}$, where $z_{\text{rel}} = z_2 - z_1$. This F_{damp} models the scenario of a resistive load connected to an EM harvester as described in Appendix A. The case of a supercapacitor as the load is considered in Appendix C. The damping force conducts infinitesimal work $dW = F_{\text{damp}}dz_{\text{rel}}$ on the quarter car with associated power $P = \frac{dW}{dt} = F_{\text{damp}}\dot{z}_{\text{rel}} = -c\dot{z}_{\text{rel}}^2$. Energy conservation then means that $c\dot{z}_{\text{rel}}^2$ is the maximal power that can be generated by the harvester in the process. The energy generated E is the instantaneous power P integrated from the moment of hitting the bump to when the motion induced by the bump stops.

The energy harvested E depends on the bump and car parameters. Unless stated otherwise, the simulations for the speed bump employ the following parameters: $c_1 = 1000 \text{ N}\cdot\text{s}/\text{m}$, $c_2 = 1400 \text{ N}\cdot\text{s}/\text{m}$, $k_1 = 5700 \text{ N}/\text{m}$, $k_2 = 135,000 \text{ N}/\text{m}$, $m_1 = 466.5 \text{ kg}$, $m_2 = 49.8 \text{ kg}$, $H = 0.1 \text{ m}$, and $L = 5.2 \text{ m}$. These were chosen to match a low-speed electric vehicle such as an E-Trike (a three-wheeled low-speed electric vehicle).

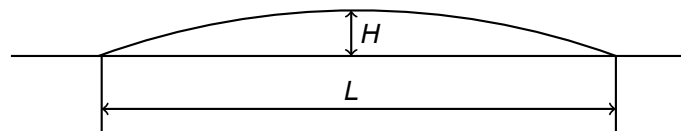


Figure 2. Speed bump model. The bump has height H and length L .

In this section on speed bumps, we use Simulink [25] to calculate the energy harvested from the relative motion of the car body and the wheel. The associated state-space model is described in Appendix A.

2.2. Most Power Is Available When Passing the Bump

In Figure 3, we see a typical output of a simulation, divided into ‘being over the bump’ (region I) and ‘having passed the bump’ (region II), respectively. The wheel is initially accelerated quickly in region I; the suspension translates this into a smoother motion of the car chassis, consistent with a significant relative motion between the chassis and wheel. It is from this relative motion that one can gain power by damping the motion with a transducer.

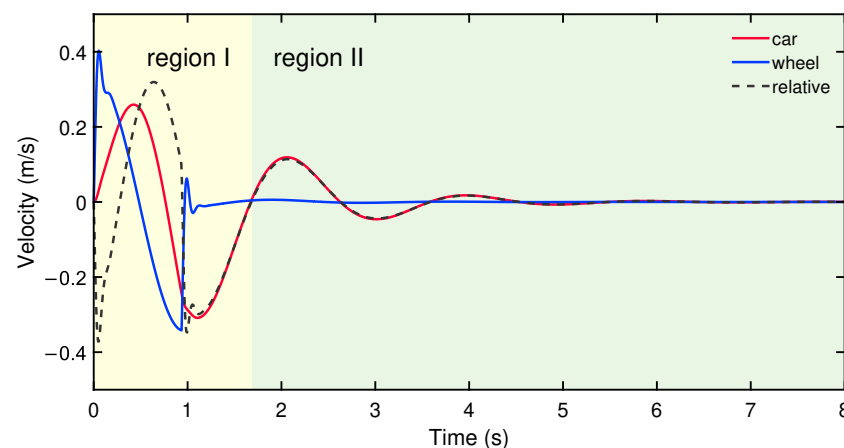


Figure 3. Quarter car velocities upon hitting speed bump. The car speed is 25 km/h. The bump is in region I, and region II starts immediately after the bump. The wheel and car body velocities are shown as well as their difference: the relative velocity.

Figure 4 shows how most energy is harvested at two moments associated with entering and exiting the bump. It moreover shows that there is a band of damping coefficients from $c = 3000 \text{ N} \cdot \text{s}/\text{m}$ to $c = 8000 \text{ N} \cdot \text{s}/\text{m}$, with higher and lower values relative to that band yielding less. Intuitively, those extreme values of c lead to the energy being dissipated in the wheel instead of being harvested.

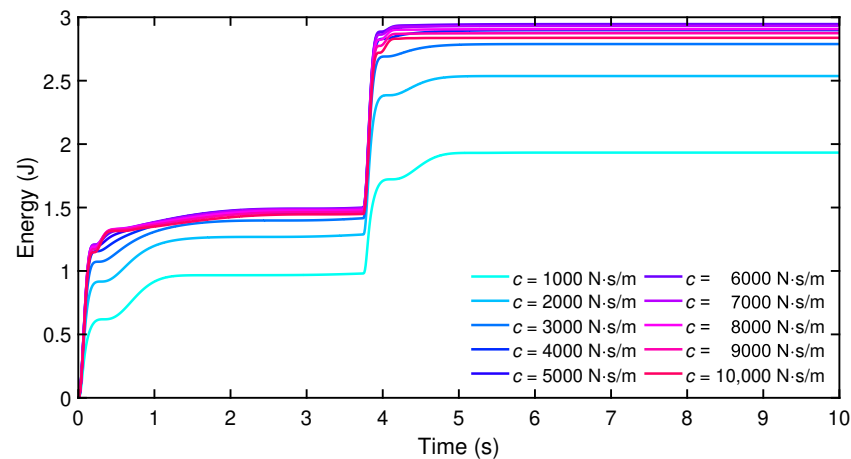


Figure 4. Most energy harvested upon entering and exiting bump. The integrated energy harvested is shown as a function of time. Here, the region after the bump is entered after around 5 s. The car speed is 5 km/h and the bump length is 5.2 m

2.3. How Harvested Power Depends on Speed, Damping Constant, and Bump Parameters

Very different values, ranging from $3000 \text{ N} \cdot \text{s}/\text{m}$ to $11,000 \text{ N} \cdot \text{s}/\text{m}$, of the damping coefficient c give rise to maximal power for different speeds, as shown in Figure 5. For example, if in the 40 km/h case c was assigned to be $3110 \text{ Ns}/\text{m}$, for which the harvested energy from a quarter car model moving at 15 km/h is maximal, the harvested energy would be 229.27 J, taking up 72.15 % of that harvested by setting $c = 11,050 \text{ N} \cdot \text{s}/\text{m}$, which is 317.75 J. The speed bump simulations show that the height of the bump has little to no effect on which c maximises the power harvested, whereas the length of the bump does (see Appendix B).

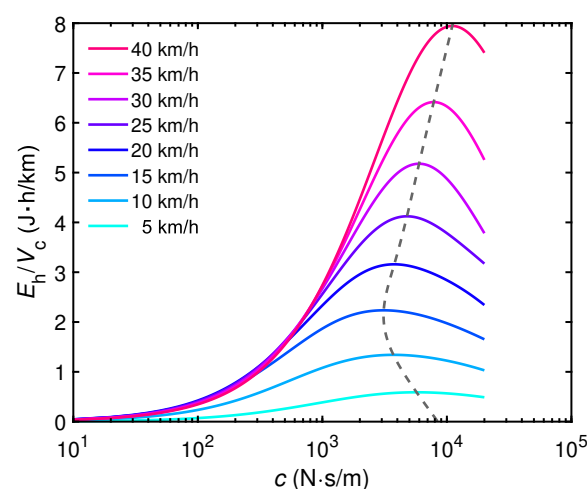


Figure 5. Impacts of c on the harvested energy at different car speeds. The harvested energy is scaled by the quarter car speed for enhancing visibility, and a dashed line connecting maximum values is included for guiding the eyes.

Next, we turn towards a road with randomly distributed bumps of varying heights and a more analytical treatment.

3. Random Road Surface

We now consider suspension energy harvesting given a road model corresponding to imperfections rather than well-structured speed bumps. A simple approach to model a random road is to pick the height $z_r(x)$ from a Gaussian distribution (also called the Bell curve or Normal distribution) at each position x (for some discretisation of x). However, physical surfaces tend to have smoother changes, so we consider a generalisation of a Gaussian road modelled by an autoregressive process, as will be explained below. We use the generalised model to derive an expression for how much power can be extracted as a function of the parameters involved. The derivation involves, for technical convenience, Fourier transforming the road surface and then working in the frequency domain.

3.1. Model of Generalised Gaussian Road AR(1)

We assume the road surface can be modelled by the autoregressive process AR(1) [26]. The term ‘autoregressive’ stems from the fact that the current value of the process is regressed upon (or predicted from) its own past values. The number 1 indicates that only the most recent time value is used. More specifically,

$$z_r(x + \Delta x) = (1 - d)z_r(x) + \zeta(0, \sigma), \quad (1)$$

where $z_r(x)$ is the height of road at position x , Δx is the distance between road height samples, d is a decay parameter, and ζ is a normal distribution function independent of x , with the mean 0 and standard deviation σ .

Applying Equation (1) iteratively n times obtains

$$z_r(x + n\Delta x) = (1 - d)^n z_r(x) + \sum_{i=0}^{n-1} (1 - d)^i \zeta_i, \quad (2)$$

where each ζ_i is picked independently with the mean 0 and standard deviation σ .

We shall later encounter ratios of the parameters d , σ , and Δx associated with the AR(1) road. We will mainly focus on the regime where d is close to 0, since we will show that the AR(1) model matches the ISO standard for characterising road roughness in that regime. We note that, for small d , two ratios of AR(1) parameters are expected to directly correspond to physical properties of the road and not be artefacts of the sampling spacing Δx . Consider replacing Δx with $n\Delta x$. Then, (i) d changes to nd for small d from Equation (2) and (ii) σ^2 changes to $n\sigma^2$. Therefore, the ratios $\lambda = \frac{d}{\Delta x}$ and $D = \frac{\sigma^2}{\Delta x}$ remain constant under such sample interval replacement. Keeping in line with common terminology of stochastic processes in physics, we term D the diffusion constant and λ the decay rate.

The impact of the road surface on the quarter car relative velocity $\dot{z}_{rel} = \frac{d}{dt}(z_1 - z_2)$ can be more conveniently calculated in terms of sinusoidal decompositions. The derivatives in the Newtonian equations of motion are easy to calculate for sinusoidal functions of time. We shall therefore make use of the Fourier transform of the road surface. To distinguish it from other heights, we shall label the road height z_r (and the heights of the two masses as z_1 and z_2 where $z_{rel} = z_1 - z_2$). Since the car travels with speed v , for time t , $z_i(x) = z_i(vt)$ whether i is 1, 2, r , or rel . There is accordingly one Fourier transform of z_i associated with the x parametrisation,

$$\hat{z}_i(\Omega) := \int_{-\infty}^{\infty} e^{-i\Omega x} z_i(x) dx \quad (3)$$

and another associated with t as follows:

$$Z_i(\omega) := \int_{-\infty}^{\infty} e^{-i\omega t} z_i(t) dt. \quad (4)$$

We shall analyse how each Fourier component of the road is associated with the Fourier component of the relative motion \dot{z}_{rel} of the same frequency. A Fourier component of the road with weight $\hat{z}_r(\Omega)$ in the Fourier decomposition will turn out to be

required by the equations of motion to have a fixed ratio with a Fourier component $\hat{z}_{\text{rel}}(\Omega)$ of the relative motion. This ratio is termed the transfer function $H(\Omega)$ of the two given Fourier components. The potential power output will be proportional to $\int |\hat{z}_{\text{rel}}(\Omega)|^2 d\Omega = \int |H(\Omega)|^2 |\hat{z}_r(\Omega)|^2 d\Omega$. We next calculate $|\hat{z}_r(\Omega)|^2$, known as the spectral power density of the road, followed by calculating the transfer function $H(\Omega)$.

3.2. Spectral Power Density of Generalised Road

We will derive the expression of the spectral power density [27] $S_{z_r}(\Omega) := |\hat{z}_r(\Omega)|^2$ for the generalised Gaussian road AR(1), where the notation “:=” denotes a definition.

We start with the fact that the spectral power density $S_{z_r}(\Omega)$ is the Fourier transform of the autocorrelation function:

$$S_{z_r}(\Omega) = \frac{1}{2\pi} \int_{-\infty}^{\infty} E(z_r(x)z_r(x+X))e^{-i\Omega X} dX, \quad (5)$$

where $E(z_r(x)z_r(x+X))$ is termed the autocorrelation of $z_r(x)$. Equation (5) follows from noting that $E[S_{z_r}(\Omega)] = E[\hat{z}_r \hat{z}_r^*] = \int_{-\infty}^{\infty} \int_{-\infty}^{\infty} e^{-i\Omega x} e^{i\Omega x'} E[z_r(x)z_r(x')]$ and from letting $x = x' + X$. (See, for example, Ref. [26] as a background reference on such calculations.)

To evaluate the integral in Equation (5) for our case of an AR(1) road, we firstly calculate the autocorrelation function. Given the AR(1) assumption of Equation (1) and recalling that the assumption implies Equation (2), the autocorrelation of the road can be obtained by

$$E[z_r(x+n\Delta x)z_r(x)] = (1-d)^{|n|} E[z_r(x)^2] = (1-d)^{|n|} \frac{\sigma^2}{1-(1-d)^2}. \quad (6)$$

The last equality in Equation (6) can be recovered as follows. $E[z_r(x+\Delta x)^2] = E[((1-d)z_r(x) + \zeta(0,\sigma))^2] = (1-d)^2 E[z_r(x)^2] + E[\zeta(0,\sigma)^2]$. Demand $E[z_r(x+\Delta x)^2] = E[z_r(x)^2] := a$. Then, $a = (1-d)^2 a + \sigma^2$, such that $a = \frac{\sigma^2}{1-(1-d)^2}$.

We now wish to use Equation (6) to evaluate Equation (5).

When $d \neq 1$, let $|n| = \frac{|X|}{\Delta x}$ and define $((1-d)^{\frac{1}{\Delta x}})^X := e^{-\alpha X}$, where $\alpha := -\frac{1}{\Delta x} \ln(1-d) > 0$. Then $(1-d)^{|n|} = e^{-\alpha|X|}$, such that the term in Equation (5) is proportional to

$$\int_{-\infty}^{\infty} e^{-\alpha|X|} e^{-i\Omega X} dX = \int_0^{\infty} e^{-\alpha X} e^{-i\Omega X} dX + \int_{-\infty}^0 e^{\alpha X} e^{-i\Omega X} dX = \frac{2\alpha}{\alpha^2 + \Omega^2}. \quad (7)$$

Thus, combining Equation (7), Equation (6) and Equation (5) one sees that

$$S_{z_r}(\Omega) = \frac{1}{2\pi} \frac{\sigma^2}{1-(1-d)^2} \frac{2\alpha}{\alpha^2 + \Omega^2} = \frac{1}{2\pi} \frac{\sigma^2}{1-e^{-2\alpha\Delta x}} \frac{2\alpha}{\alpha^2 + \Omega^2}. \quad (8)$$

When $d = 1$, from Equation (1), we have $z(x) = \zeta(0,\sigma)$, which corresponds to white noise. A white noise road profile has distribution $N(0,\sigma)$ and is commonly stated as having autocorrelation $\sigma^2\delta(X)$ (where $\delta(X)$ is the unit impulse function), such that

$$\begin{aligned} S_z(\Omega) &= \frac{1}{2\pi} \int_{-\infty}^{\infty} E(z(x)z(x+X))e^{-i\Omega X} dX \\ &= \frac{1}{2\pi} \int_{-\infty}^{\infty} \sigma^2\delta(X)e^{-i\Omega X} dX \\ &= \frac{1}{2\pi} \sigma^2 \int_{-\infty}^{\infty} \delta(X)(\cos(\Omega X) - i\sin(\Omega X)) dX \\ &= \frac{1}{2\pi} \sigma^2 (\cos(0) - i\sin(0)) \\ &= \frac{\sigma^2}{2\pi}. \end{aligned} \quad (9)$$

Equation (9) can, reassuringly, also be recovered as a limit of the following computationally well-defined *discrete* Fourier transform of Equation (6):

$$\int_{-\infty}^{\infty} (1-d)^{|n|} \frac{\sigma^2}{1-(1-d)^2} e^{-i\Omega X} dX \approx \frac{\sigma^2}{1-(1-d)^2} \sum_{n=-\infty}^{\infty} (1-d)^{|n|} e^{-i\Omega \Delta x n} \quad (10)$$

$$= \left(\frac{\sigma^2}{1-(1-d)^2} \right) \left(\frac{1}{1+(1-d)^2 - 2(1-d)\cos(\Omega \Delta x)} \right)$$

From Equation (10), when $d = 1$, $S_{z_r} = \frac{\sigma^2}{2\pi}$.

3.3. Relation to ISO Standard for Characterising Road Roughness

In the ISO 8608 standard, the road profile is characterised in terms of the power density spectral density $S_{z_r}(\Omega)$ [21] as a function of the spatial angular frequency Ω . If we again let x represent the longitudinal position of the vehicle and z_x represent the road height above the reference line at x , then $\hat{z}(\Omega) := \int_{-\infty}^{\infty} e^{-i\Omega x} z_r(x) dx$ and $S_{z_r}(\Omega) := |\hat{z}(\Omega)|^2$, where ‘:=’ denotes a definition. The ISO 8608 standard [21] involves the curve-fitting assumption that

$$S_{z_r}(\Omega) = C \left(\frac{\Omega}{\Omega_0} \right)^{-\mathcal{W}} \quad \text{if } 2\pi \cdot 0.011 \leq \Omega \leq 2\pi \cdot 2.83 \text{ rad/m, and 0 otherwise.} \quad (11)$$

Here, Ω is the spatial angular frequency, and often $\Omega_0 = 1$ rad/m. C is a coefficient that can be interpreted as the road roughness. The ‘waviness’ \mathcal{W} is a somewhat controversial value, which may depend on Ω and is often set as 2 for simplicity [28]. The formula for $S_{z_r}(\Omega)$ then only has one free parameter, which is the roughness coefficient C .

We are now in a position to derive $S_{z_r}(\Omega)$ of Equation (11) from the assumption of the road being generated by AR(1), as defined in Equation (1).

For a small decay rate, $\lambda = \frac{d}{\Delta x}$, $\alpha \approx \frac{d}{\Delta x}$, and $1 - (1-d)^2 \approx 2d$. Then, from Equation (8),

$$S_{z_r}(\Omega) = \frac{1}{2\pi} \frac{\sigma^2}{1-(1-d)^2} \frac{2\alpha}{\alpha^2 + \Omega^2} \approx \frac{1}{2\pi} \frac{\sigma^2}{2d} \frac{2\frac{d}{\Delta x}}{\left(\frac{d}{\Delta x}\right)^2 + \Omega^2} \approx \frac{1}{2\pi} \frac{\sigma^2}{\Delta x} \Omega^{-2} = \frac{D}{2\pi} \Omega^{-2}, \quad (12)$$

where the second approximation assumes that $\Omega^2 \gg \frac{d}{\Delta x}$. D is the diffusion rate of the road. When comparing with Equation (11), we find that the road roughness coefficient of ISO 8608 and the diffusion coefficient of the AR(1) road are equal up to a factor:

$$C = \frac{D}{2\pi}. \quad (13)$$

4. Energy Harvested on a Random Road Surface

We firstly derive the transfer function which captures how different the frequency components of the road surface are associated with the relative motion of the car body and wheel. We then use the transfer function to derive the power dissipated as a function of the car and road parameters.

4.1. Transfer Function on a Gaussian Road

Transfer functions play a crucial role in analysing and optimising suspension systems (see, for example, Ref. [17]). For a given sinusoidal input with a given frequency, there is a certain output response of the given frequency, and the transfer function in question is the ratio of the output and input amplitudes. In our case, the input is the road surface and the output is the relative motion of the car body and tire.

The relevant transfer function of the quarter car model can be derived as follows. Firstly, write down the Newtonian equations of motion for the quarter car:

$$\begin{cases} m_1 \ddot{z}_1 = k_1(z_2 - z_1) + c_1(\dot{z}_2 - \dot{z}_1) \\ m_2 \ddot{z}_2 = k_2(z_r - z_2) + c_2(\dot{z}_r - \dot{z}_2) - k_1(z_2 - z_1) - c_1(\dot{z}_2 - \dot{z}_1), \end{cases} \quad (14)$$

where the terms are as defined in Figure 1. Fourier transforming both sides, and writing for notational simplicity $\mathcal{F}[z_i(t)] = Z_i(\omega)$, yields

$$\begin{cases} -m_1\omega^2 Z_1(\omega) = k_1(Z_2(\omega) - Z_1(\omega)) + i\omega c_1(Z_2(\omega) - Z_1(\omega)) \\ -m_2\omega^2 Z_2(\omega) = k_2(Z_r(\omega) - Z_2(\omega)) + i\omega c_2(Z_r(\omega) - Z_2(\omega)) \\ \quad - k_1(Z_2(\omega) - Z_1(\omega)) - i\omega c_1(Z_2(\omega) - Z_1(\omega)) \end{cases} \quad (15)$$

Equation (15) can be seen in a few lines (see Appendix E) to yield a transfer function $H(\omega)$, respecting

$$\begin{aligned} H(\omega) &:= \frac{Z_2(\omega) - Z_1(\omega)}{Z_r(\omega)} = \frac{-m_1\omega^2}{-m_1\omega^2 + k_1 + i\omega c_1} \frac{Z_2(\omega)}{Z_r(\omega)} \\ &= \frac{-m_1\omega^2(k_2 + i\omega c_2)}{(-m_1\omega^2 + k_1 + i\omega c_1)(-m_2\omega^2 + k_2 + i\omega c_2) - m_1\omega^2(k_1 + i\omega c_1)}. \end{aligned} \quad (16)$$

Equation (16) corresponds to a resistive load coupled to the EM harvester. In Appendix C, we moreover derive an alternative transfer function H corresponding to a supercapacitor as a load.

We can now write down the transfer function for a common choice of car parameters. The *golden car* is a quarter car model used in the international road roughness index (see Appendix D) with specific parameter values given in Table 1. Taking that case as an example, Equation (16) reduces to

$$H_{\text{gold}}(\omega) = \frac{-\omega^2 \kappa_2}{(\kappa_1 + i\omega c_{\text{gold}} - \omega^2)(\kappa_2 - \omega^2 \mu) - (\kappa_1 + i\omega c_{\text{gold}})\omega^2}, \quad (17)$$

where the golden car parameters are denoted as $\mu = m_2/m_1$, $\kappa_1 = k_1/m_1$, $\kappa_2 = k_2/m_1$, $c_{\text{gold}} = c_1/m_1$, and $c_0 = c_2/m_1 = 0$ [29].

Table 1. Parameters of the *golden car*.

Parameter	Value	Unit
$\mu = m_2/m_1$	0.15	-
$\kappa_1 = k_1/m_1$	63.3	s ⁻²
$\kappa_2 = k_2/m_1$	653	s ⁻²
$c_{\text{gold}} = c_1/m_1$	6.0	s ⁻¹
$c_0 = c_2/m_1$	0.0	s ⁻¹

The power density spectrum of the relative motion of the golden quarter car is, for any quarter car, given in terms of the power density spectrum

$$S_{z_{\text{rel}}}(\Omega) = \left| \frac{Z_2(\omega) - Z_1(\omega)}{Z_r(\omega)} Z_r(\omega) \right|^2 = |H(\Omega)|^2 S_{z_r}(\Omega). \quad (18)$$

Next, we will apply Equation (17) and Equation (18) to calculate the energy dissipation in the damper/harvester.

4.2. Potential Power Output

The instantaneous power dissipated in the damper/harvester can be written in terms of the relative motion of the tire and car body as $P = F\dot{z}_{\text{rel}} = (c_1\dot{z}_{\text{rel}})\dot{z}_{\text{rel}} = c_1\dot{z}_{\text{rel}}^2$. Taking the stochastic average yields

$$E[P] = c_1 E[\dot{z}_{\text{rel}}^2] = c_1 \sigma_{\dot{z}_{\text{rel}}}^2, \quad (19)$$

where the second equality assumes that the average relative velocity, without conditioning on known previous values, is 0.

$$\sigma_{z_{\text{rel}}}^2 = \int_{-\infty}^{+\infty} \omega^2 S_{z_{\text{rel}}}(\omega) d\omega. \quad (20)$$

Moreover,

$$S_{z_{\text{rel}}}(\omega) = |H_{\text{rel}}(\omega)|^2 S_{z_r}(\omega) \quad (21)$$

Moreover, noting that

$$S_{z_r}(\omega) = \frac{1}{v} S_{z_r}(\Omega), \quad (22)$$

and, as shown earlier, the known fact that

$$S_{z_r}(\Omega) = \frac{1}{2\pi} \int_{-\infty}^{\infty} E(z_r(x)z_r(x+X))e^{-i\Omega X} dX, \quad (23)$$

one sees that $\sigma_{z_{\text{rel}}}^2$ can be written as

$$\begin{aligned} \sigma_{z_{\text{rel}}}^2 &= \int_{-\infty}^{+\infty} S_{z_{\text{rel}}}(\omega) d\omega \\ &= \frac{1}{2\pi v} \int_{-\infty}^{+\infty} \omega^2 \left(\int_{-\infty}^{\infty} E(\xi(x)\xi(x+X))e^{-i\Omega X} dX \right) |H_{\text{rel}}(\omega)|^2 d\omega. \end{aligned} \quad (24)$$

Plugging Equation (8) and Equation (16) into Equation (24) yields

$$\begin{aligned} \sigma_{z_{\text{rel}}}^2 &= \frac{1}{2\pi v} \int_{-\infty}^{+\infty} \omega^2 \left(\frac{\sigma^2}{1 - (1-d)^2 \alpha^2 + (\omega/v)^2} \right) \\ &\quad \left(\frac{d\omega m_1^2 (k_2^2 + \omega^2 c_2^2) \omega^4}{(m_1 m_2 \omega^4 - (m_1 k_2 + m_2 k_1 + c_1 c_2 + m_1 k_1) \omega^2 + k_1 k_2)^2 + ((-m_1 c_2 - m_2 c_1 - m_1 c_1) \omega^3 + (c_2 k_1 + c_1 k_2) \omega)^2} \right) d\omega \end{aligned} \quad (25)$$

By putting in, for example, the golden car parameters, Equation (25) becomes

$$\begin{aligned} \sigma_{z_{\text{rel}}}^2 &= \frac{1}{2\pi v} \int_{-\infty}^{+\infty} \omega^2 \left(\frac{\sigma^2}{1 - (1-d)^2 \alpha^2 + (\omega/v)^2} \right) \\ &\quad \left(\frac{426409 s^{-2} \omega^4}{(0.15 \omega^4 - (725.795 s^{-2}) \omega^2 + 41334.9 s^{-4})^2 + (6.9 s^{-1} \omega^3 + (3918 s^{-3}) \omega)^2} \right) d\omega \end{aligned} \quad (26)$$

Furthermore, for the golden car speed used in the IRI road roughness index, $v = 22.22$ m/s, the integral of Equation (26) can be evaluated analytically with Mathematica to yield

$$\begin{aligned} \sigma_{z_{\text{rel}}}^2 &= \left(\frac{\sigma^2}{1 - (1-d)^2} \right) \left(\frac{2142.66\alpha - 25732.7\alpha^3 + 173379\alpha^5 + 16738.4\alpha^7}{1.27791 + 16.4885\alpha^2 + 108.163\alpha^4 + 15.3164\alpha^6 + \alpha^8} \right) \\ &\approx \left(\frac{\sigma^2}{2} \right) 1676.69 \frac{1}{\Delta x} = \frac{D}{2} 1676.69 \end{aligned} \quad (27)$$

where α is defined as $\alpha = -\frac{1}{\Delta x} \ln(1-d)$ and $D := \frac{\sigma^2}{\Delta x}$ is the diffusion constant of the AR(1) process. For concreteness, suppose $D = \frac{0.01^2}{10}$ and that the golden car parameters are used. For a golden car with $m_1 = 500$ kg, the energy dissipated from Equation (19) is then

$$P = c_1 \sigma_{z_{\text{rel}}}^2 = c_1 \left(\frac{D}{2} 1676.69 \right)^2 = 6 * 500 * (9.156 * 0.01)^2 = 25.15 \text{ W}. \quad (28)$$

The above argument exemplifies how, in general, plugging Equation (25) into Equation (19) yields an analytical expression for the expected power as a function of the parameters of the quarter car model and the AR(1) road model. This is a key technical contribution of this paper.

We can also, as a further example, evaluate the power when the road model reduces to AR(0). From Equation (8), the power spectrum is then $\frac{\sigma^2}{2\pi}$. Similar to Equation (26),

$$\begin{aligned} & \sigma_{z_{\text{rel}}}^2 \\ &= \frac{\sigma^2}{2\pi v} \int_{-\infty}^{+\infty} \omega^2 \left(\frac{426409s^{-2}\omega^4 d\omega}{(0.15\omega^4 - (725.795s^{-2})\omega^2 + 41334.9s^{-4})^2 + (6.9s^{-1}\omega^3 + (3918s^{-3})\omega)^2} \right) \\ & \approx 91.485\sigma^2, \end{aligned} \quad (29)$$

which leads to the power of the golden car of $m_1 = 500$ kg and $\sigma = 0.01$ m to be

$$P = c_1 \sigma_{z_{\text{rel}}}^2 = 6 * 500 * 91.485 * 0.01^2 = 27.45 \text{ W} \quad (30)$$

The golden car example can further be used to relate the International Roughness Index IRI for roads [29,30] to the extractable power of that golden car, as detailed in Appendix D.

5. Summary and Outlook

We investigated how much power can be harvested from the suspension of a vehicle. We assumed the paradigm of converting the energy otherwise dissipated as heat into work. We firstly investigated how much power can be harvested from a semicircular speed bump, finding that most power is harvested whilst passing the bump rather than in the oscillations after it, and that the harvested amount depends on the relation between the damping coefficient to the speed and the length of the bump. We then proposed a generalised Gaussian stochastic model for roads: AR(1). Under the AR(1) assumption, we derived an analytical expression for the amount of power that can be extracted as a function of the parameters of the car and road model. For a special case of AR(1) and a standard car known as the golden car, the extractable power can be directly determined from the International Roughness Index of the road. Another special case of AR(1) allows us to derive a key assumption underlying an ISO standard for characterising road roughness, such that parameters from the ISO standard, together with a free parameter of AR(1), can be employed to analytically calculate the extractable power.

Our findings should help evaluate the potential for energy harvesting from vehicle suspension across a range of road conditions. The results also suggest that the standard characterisations of roads should be augmented to include both free parameters in the AR(1) model. Furthermore, preliminary results not described here suggest that convolutional neural networks can significantly enhance the harvesting by controlling the damping coefficient efficiently, something which deserves further investigation. In particular, dynamically varying damping parameters should be investigated. Furthermore, the assumption of linear systems could be relaxed. Our analytical methods should be extended to more complicated non-linear damping forces from the harvester. The analytical results here should be compared with experimental data. The investigation can also be viewed as contributing to the general program of understanding how much power can be extracted from pseudo-random power sources [31,32].

Author Contributions: Conceptualization, O.D. and D.E.; methodology, H.G., W.Z.; software, W.Z. and H.G.; validation, O.D., D.E. and F.M.; formal analysis, H.G.; resources, O.D.; writing—original draft preparation, H.G. and W.Z.; writing—review and editing, O.D., F.M. and D.E.; supervision, O.D. All authors have read and agreed to the published version of the manuscript.

Funding: We acknowledge support from the National Natural Science Foundation of China (Grants No. 12050410246, No. 1200509, No. 12050410245), City University of Hong Kong (Project No. 9610623) and the Shenzhen Science Technology and Innovation Commission (Grant No. 20200805101139001)

Informed Consent Statement: Not applicable.

Data Availability Statement: All relevant data is shown in the article.

Acknowledgments: We thank Hessner Technologies Limited in HK Science Park, Pietro Mincuzzi at Troublemaker and Emil Jersling for discussions concerning energy harvesting from suspension of low-speed electric vehicles.

Conflicts of Interest: The authors declare no conflicts of interest.

Abbreviations

Symbol	Description
v	Speed of the car
c_1	Damping coefficient of the suspension
c	Damping coefficient of the suspension $c = c_1$
c_2	Damping coefficient of the tire
F_{damp}	Damping force of the suspension
z_1	z coordinate of the car body
z_2	z coordinate of the tire
z_{rel}	Relative displacement between the car body and the tire
z_r	z coordinate of the road
$\hat{z}_i(\Omega)$	Fourier transformation of $z_i(x)$ in the spatial angular frequency domain, $i = 1, 2, r, \text{rel}$
$Z_i(\omega)$	Fourier transformation of $z_i(t)$ in the temporal angular frequency domain, $i = 1, 2, r, \text{rel}$
m_1	Mass of the car body
m_2	Mass of the tire
k_1	Spring constant of the suspension
k_2	Spring constant of the tire
H	Height of the speed bump
$H(\omega)$	Transfer function
L	Length of the speed bump
W	Work conducted on the suspension
P	Power of the suspension damping
S_{z_r}	Spectral power density function
Ω	Spatial angular frequency
ω	Temporal angular frequency
C	Road roughness
\mathcal{W}	Road waviness
$\xi(0, \sigma)$	Normal distributed random variable with mean 0 and variance σ
d	A decay parameter used in AR(1) Gaussian road
σ	Variance
α	$= -\frac{1}{\Delta x} \ln(1 - d)$
Δx	Sampling distance of the Gaussian road
λ	Decay rate of the AR(1) Gaussian road
D	Diffusion constant for the AR(1) Gaussian road
μ	$= m_2/m_1$ for the golden car
κ_1	$= k_1/m_1$ for the golden car
κ_2	$= k_2/m_1$ for the golden car
c_{gold}	$= c_1/m_1$ for the golden car
c_0	$= c_2/m_1$ for the golden car

Appendix A. State Space Model of Quarter Car

Appendix A.1. State-Space Model of Vertical Car Body Motion

Differential equations of the quarter car model:

$$\begin{cases} m_1 \ddot{z}_1 + c_1 \dot{z}_1 - c_1 \dot{z}_2 + k_1 z_1 - k_1 z_2 = 0 \\ m_2 \ddot{z}_2 + (c_1 + c_2) \dot{z}_2 - c_1 \dot{z}_1 + (k_1 + k_2) z_2 - k_1 z_1 = c_2 \dot{z}_r + k_2 z_r \end{cases}$$

The state vector $\vec{z}(t) = \begin{bmatrix} \dot{z}_1 \\ \dot{z}_2 \\ z_1 \\ z_2 \end{bmatrix}$, and the State-space model can be written as

$$\dot{\vec{z}}(t) = \begin{bmatrix} -\frac{c_1}{m_1} & \frac{c_1}{m_1} & -\frac{k_1}{m_1} & \frac{k_1}{m_1} \\ \frac{c_1}{m_2} & -\frac{c_1+c_2}{m_2} & \frac{k_1}{m_2} & -\frac{k_1+k_2}{m_2} \\ 0 & 0 & 1 & 0 \\ 0 & 0 & 0 & 1 \end{bmatrix} \vec{z}(t) + \begin{bmatrix} 0 & 0 \\ \frac{c_2}{m_2} & \frac{k_2}{m_2} \\ 0 & 0 \\ 0 & 0 \end{bmatrix} \begin{bmatrix} \dot{z}_r \\ z_r \end{bmatrix}.$$

State-Space Model with Harvester

In this model, we assume that an electromagnetic harvester is installed between car body and wheel and harvesting energy from the relative motion of the two parts. An example model for the instantaneous electrical power generated by the system is [33]

$$P_i = \frac{(NBl)^2}{R_L + R_c + j\omega L_c} (\dot{z}_1 - \dot{z}_2)^2,$$

where

- N — turns of coil
- B — average flux density in the air-gap
- l — effective length of coil
- R_L — resistance of load
- R_c — resistance of coil
- L_c — inductance of coil
- j — imaginary unit
- ω — angular frequency of relative motion.

Assuming that the contribution from the inductance of the coil is negligible, this can be simplified as

$$P_i = c(\dot{z}_1 - \dot{z}_2)^2.$$

Appendix B. Different Bump Lengths

Consider that the height of the speed bump is $H = 0.2$ m. The bump length is set to be 1, 2, 3, 4, 5, and 6 m, respectively. The quarter car is moving at 20 km/h.

From Figure A1, a strong dependence between which c maximises the power output and the length of the speed bump are observed.

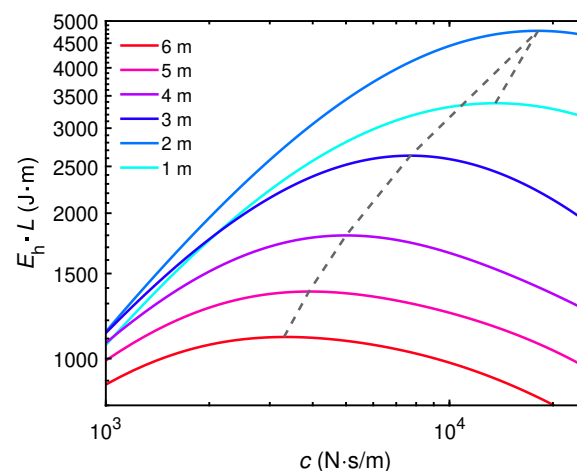


Figure A1. Impacts of c on harvested energy for different bump lengths L (1–6 m). The harvested energy is scaled by the bump length for enhancing visibility, and a dashed line connecting maximum values is included for guiding the eyes.

Appendix C. Em Harvester Coupled with a Supercapacitor

We now consider what change of the load is not resistive, but a supercapacitor. This is motivated by low-speed electric vehicle applications. The simplified set-up we consider is depicted in Figure A2.

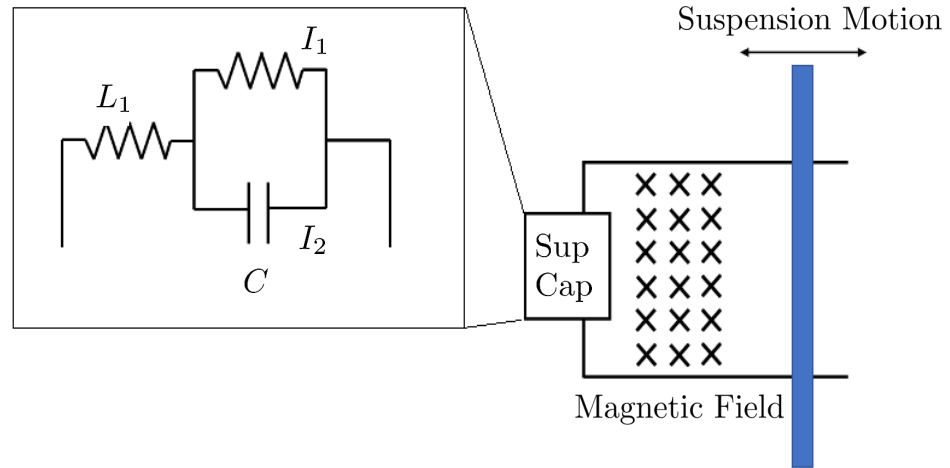


Figure A2. A simplified EM harvester circuit. The rod cutting the magnetic induction line has a velocity proportional to the relative velocity of the tire and chassis. The generated electric energy is stored in a supercapacitor for quick charging and discharging.

We firstly write down the equations governing the time evolution. f is the force from the supercapacitor and harvester onto the tyre and chassis. Capital letters indicate Fourier transform, e.g., F is the Fourier transform of f .

$$\begin{aligned}
 m_1 \ddot{z}_1 &= (z_2 - z_1)k_1 + f \\
 m_2 \ddot{z}_2 &= (z_r - z_2)k_2 + (\dot{z}_r - \dot{y}_2)c_2 - ((z_2 - z_1)k_1 + f) \\
 f &= NIBl \\
 \varepsilon &= N(\dot{z}_2 - \dot{z}_1)BL \\
 I &= I_1 + I_2 \\
 \varepsilon &= L_1 \frac{dI}{dt} + L_2 \frac{dI_2}{dt} \\
 L_2 \frac{dI_2}{dt} &= \frac{1}{C} \int_0^t I_1 dt
 \end{aligned} \tag{A1}$$

Fourier transforming the EM force f gives

$$F = -iN^2B^2l^2 \frac{1 - \omega^2CL_2}{\omega[L_1(1 - \omega^2CL_2) + L_2]} Z_1 := -im_1\gamma(\omega)Z_1 \tag{A2}$$

where

$$\gamma(\omega) := \frac{N^2B^2l^2}{m_1} \frac{1 - \omega^2CL_2}{\omega[L_1(1 - \omega^2CL_2) + L_2]}. \tag{A3}$$

We now, armed with the Fourier transform of f , return to the equations of motion. Firstly, we rewrite them as

$$\begin{aligned}
 m_1 m_2 \ddot{z}_2 &= (z_2 - z_1)k_1 m_2 + f m_2 \\
 m_1 m_2 \ddot{z}_2 &= (z_r - z_2)k_2 m_1 + (\dot{z}_r - \dot{z}_2)c_2 m_1 - ((z_2 - z_1)k_1 + f)m_1
 \end{aligned} \tag{A4}$$

Simplifying and Fourier transforming gives

$$\begin{aligned} -\omega^2 m_1 m_2 Z_1 &= -Z_1 k_1 (m_2 + m_1) + \gamma(\omega) (m_1 + m_2) Z_1 + Z_2 k_2 m_1 + i\omega Z_2 c_2 m_1 \\ -\omega^2 m_1 m_2 Z_2 &= -Z_2 k_2 m_1 - i\omega Z_2 c_2 m_1 + (Z_1 k_1 - \gamma(\omega) Z_1) m_1 + \omega^2 m_1 m_2 Z_r, \end{aligned} \quad (\text{A5})$$

which may be abbreviated as

$$\begin{aligned} aZ_1 &= bZ_2 \\ cZ_2 &= dZ_1 + eZ_r, \end{aligned} \quad (\text{A6})$$

such that the transfer function of interest is

$$\begin{aligned} H(\omega) &= \frac{Z_1 - Z_2}{Z_r} \\ &= \frac{Z_1(1 - \frac{a}{b}e)}{cZ_2 - dZ_1} = \frac{1 - \frac{a}{b}}{c\frac{a}{b} - d}. \end{aligned} \quad (\text{A7})$$

Appendix D. IRI Relation To Power

The International Roughness Index (IRI) is a common indicator of pavement roughness. It is defined as the difference between the total displacement L (in meters) of the body suspension and the driving distance, in kilometers, of the golden car standard vehicle driving at the speed of $V = 80$ km/h [29,30]: $\text{IRI} = \frac{1}{L} \int_0^{L/V} |\dot{z}_{\text{rel}}| dt$.

The IRI is closely related to the integral of the power dissipated $P = c|\dot{z}_{\text{rel}}|^2$, but there is a subtlety in that IRI uses the absolute value without the power of 2.

We make the significant assumption that $|\dot{z}_{\text{rel}}|$ is approximately identically and independently distributed such that $E(\int_0^{L/V} |\dot{z}_{\text{rel}}| dt) \approx E(|\dot{z}_{\text{rel}}|) \frac{L}{V}$. This assumption is for mathematical convenience but can be physically justified in a regime where the suspension response time is much faster than the road variations.

Let $|\dot{z}_{\text{rel}}| := l$ for notational simplicity, then

$$E[|l|] = \int_{-\infty}^{\infty} \rho(l) |l| dl \quad (\text{A8})$$

$$= \int_0^{\infty} (\rho(l) + \rho(-l)) l dl \quad (\text{A9})$$

$$= \int_{l=0}^{\infty} 2\rho(l) l dl \quad (\text{A10})$$

$$= \frac{2}{\sigma_l \sqrt{2\pi}} \int_{l=0}^{\infty} e^{-\frac{l^2}{2\sigma_l^2}} l dl \quad (\text{A11})$$

$$= \frac{2}{\sigma_l \sqrt{2\pi}} \sigma_l^2 \quad (\text{A12})$$

$$= \frac{2\sigma_l}{\sqrt{2\pi}}. \quad (\text{A13})$$

Thus, taking into account the definition $\text{IRI} = \frac{1}{L} \int_0^{L/V} |\dot{z}_{\text{rel}}| dt$ [29,30], we find $E[\text{IRI}] = \frac{2\sigma_l}{v\sqrt{2\pi}}$ where $|\dot{z}_{\text{rel}}| := l$.

$$c_{\text{gold}} \frac{\pi v^2}{2} \text{IRI}^2 = c_{\text{gold}} \sigma_{\dot{z}_{\text{rel}}}^2 = P, \quad (\text{A14})$$

$c_{\text{gold}} \frac{\pi v^2}{2} = 4653.28 m_1$, and the IRI of airport runways, for example, is $\text{IRI} < 2 \times 10^{-3}$, and for rough roads is $\text{IRI} > 8 \times 10^{-3}$.

Although the derivation of Equation (A14) includes a strong i.i.d. assumption, numerics suggest that the equation holds arbitrarily well for AR(0) roads, indicating that it should be possible to derive Equation (A14) without that strong assumption.

Appendix E. Transfer Function Given AR(1) Road Details

The transfer function of the quarter car model can be derived as below. The motion equation of quarter car is

$$\begin{cases} m_1 \ddot{z}_1 = k_1(z_2 - z_1) + c_1(\dot{z}_2 - \dot{z}_1) \\ m_2 \ddot{z}_2 = k_2(z_r - z_2) + c_2(\dot{z}_r - \dot{z}_2) - k_1(z_2 - z_1) - c_1(\dot{z}_2 - \dot{z}_1). \end{cases} \quad (\text{A15})$$

Taking the Fourier transformation of both sides and defining $\mathcal{F}[z_i(t)] = Z_i(\omega)$, we have

$$\begin{cases} -m_1 \omega^2 Z_1(\omega) = k_1(Z_2(\omega) - Z_1(\omega)) + i\omega c_1(Z_2(\omega) - Z_1(\omega)) \\ -m_2 \omega^2 Z_2(\omega) = k_2(U(\omega) - Z_2(\omega)) + i\omega c_2(U(\omega) - Z_2(\omega)) \\ \quad - k_1(Z_2(\omega) - Z_1(\omega)) - i\omega c_1(Z_2(\omega) - Z_1(\omega)). \end{cases} \quad (\text{A16})$$

When simplifying it, we obtain

$$\begin{cases} (-m_1 \omega^2 + k_1 + i\omega c_1)Z_1(\omega) = (k_1 + i\omega c_1)Z_2(\omega) \\ (-m_2 \omega^2 + k_1 + k_2 + i\omega c_1 + i\omega c_2)Z_2(\omega) = (k_2 + i\omega c_2)U(\omega) + (k_1 + i\omega c_1)Z_1(\omega). \end{cases} \quad (\text{A17})$$

When solving the above equations, we obtain

$$\begin{cases} Z_1(\omega) = \frac{k_1 + i\omega c_1}{-m_1 \omega^2 + k_1 + i\omega c_1} Z_2(\omega) \\ Z_2(\omega) = \frac{(k_2 + i\omega c_2)(-m_1 \omega^2 + k_1 + i\omega c_1)}{(-m_1 \omega^2 k_1 + i\omega c_1)(-m_2 \omega^2 + k_2 + i\omega c_2) - m_1 \omega^2 (k_1 + i\omega c_1)}. \end{cases} \quad (\text{A18})$$

The energy harvested by the suspension is directly related to the relative displacement between the car body and the tire, $|z_2(t) - z_1(t)|$. Then, we calculate the transfer function $H(\omega)$ that tells us the relative displacement $Z_2(\omega) - Z_1(\omega)$ based on the road profile $Z_r(\omega)$,

$$\begin{aligned} H(\omega) &= \frac{Z_2(\omega) - Z_1(\omega)}{Z_r(\omega)} = \frac{-m_1 \omega^2}{-m_1 \omega^2 + k_1 + i\omega c_1} \frac{Z_2(\omega)}{Z_r(\omega)} \\ &= \frac{-m_1 \omega^2 (k_2 + i\omega c_2)}{(-m_1 \omega^2 + k_1 + i\omega c_1)(-m_2 \omega^2 + k_2 + i\omega c_2) - m_1 \omega^2 (k_1 + i\omega c_1)}. \end{aligned} \quad (\text{A19})$$

References

- Holdren, J.P. Population and the energy problem. *Popul. Environ.* **1991**, *12*, 231–255. [[CrossRef](#)]
- Priya, S.; Inman, D.J. *Energy Harvesting Technologies*; Springer: Berlin/Heidelberg, Germany, 2009; Volume 21.
- Hrovat, D. Survey of advanced suspension developments and related optimal control applications. *Automatica* **1997**, *33*, 1781–1817. [[CrossRef](#)]
- Wei, C.; Jing, X. A comprehensive review on vibration energy harvesting: Modelling and realization. *Renew. Sustain. Energy Rev.* **2017**, *74*, 1–18. [[CrossRef](#)]
- Abdelkareem, M.A.A.; Xu, L.; Ali, M.K.A.; Elagouz, A.; Mi, J.; Guo, S.; Liu, Y.; Zuo, L. Vibration energy harvesting in automotive suspension system: A detailed review. *Appl. Energy* **2018**, *229*, 672–699. [[CrossRef](#)]
- Li, S.; Xu, J.; Pu, X.; Tao, T.; Gao, H.; Mei, X. Energy-harvesting variable/constant damping suspension system with motor based electromagnetic damper. *Energy* **2019**, *189*, 116199. [[CrossRef](#)]
- Karnopp, D. Active and semi-active vibration isolation. In *Current Advances in Mechanical Design and Production VI*; Elarabi, M.E., Wifi, A.S., Wifi, A.S., Eds.; Pergamon: Oxford, UK, 1995; pp. 409–423.
- Suda, Y.; Nakadai, S.; Nakano, K. Hybrid suspension system with skyhook control and energy regeneration (development of self-powered active suspension). *Veh. Syst. Dyn.* **1998**, *29* (Suppl. 1), 619–634. [[CrossRef](#)]
- Okada, Y.; Harada, H. Regenerative control of active vibration damper and suspension systems. In Proceedings of the 35th IEEE Conference on Decision and Control, Kobe, Japan, 13 December 1996; IEEE: Piscataway, NJ, USA, 1996; Volume 4, pp. 4715–4720.
- Zhang, Z.; Zhang, X.; Rasim, Y.; Wang, C.; Du, B.; Yuan, Y. Design, modelling and practical tests on a high-voltage kinetic energy harvesting (eh) system for a renewable road tunnel based on linear alternators. *Appl. Energy* **2016**, *164*, 152–161. [[CrossRef](#)]
- Hoo, G.K. Investigation of Direct-Current Brushed Motor Based Energy Regenerative Automotive Damper. Master Thesis, Department Mechanical Engineering, National University of Singapore, Singapore, 2013.

12. Faiz, J.; Ebrahimi-Salari, M.; Shahgholian, G. Reduction of cogging force in linear permanent-magnet generators. *IEEE Trans. Magn.* **2009**, *46*, 135–140. [[CrossRef](#)]
13. 2006. Available online: <https://www.speedgoat.com/success-stories/speedgoat-user-stories/clearmotion> (accessed on 5 August 2024).
14. 2006. Available online: www.audi-mediacenter.com/en/photos/detail/the-innovative-shock-absorber-system-from-audi-new-technology-saves-fuel-and-enhances-comfort-36880 (accessed on 5 August 2024).
15. Zuo, L.; Zhang, P.-S. Energy harvesting, ride comfort, and road handling of regenerative vehicle suspensions. *J. Vib. Acoust.* **2013**, *135*, 011002. [[CrossRef](#)]
16. Fairbanks, J. Vehicular thermoelectrics: A new green technology. In Proceedings of the 2011 Directions in Engine-Efficiency and Emissions Research (DEER) Conference, Detroit, MI, USA, Coronado, CA, USA, 3–8 January 2011.
17. Karnopp, D.C.; Margolis, D.L.; Rosenberg, R.C. *System dynamics: Modeling, Simulation, and Control of Mechatronic Systems*; John Wiley & Sons: Hoboken, NJ, USA, 2012.
18. Türkyay, S.; Akçay, H. A study of random vibration characteristics of the quarter-car model. *J. Sound Vib.* **2005**, *282*, 111–124. [[CrossRef](#)]
19. Alleyne, A.; Hedrick, J.K. Nonlinear control of a quarter car active suspension. In Proceedings of the 1992 American Control Conference, Chicago, IL, USA, 24–26 June 1992; IEEE: Piscataway, NJ, USA, 1992; pp. 21–25.
20. Box, G.E.P.; Jenkins, G.M.; Reinsel, G.C.; Ljung, G.M. *Time Series Analysis: Forecasting and Control*; John Wiley & Sons: Hoboken, NJ, USA, 2015.
21. *ISO8608; Mechanical Vibration—Road Surface Profiles—Reporting of Measured Data*. Standard, International Organization for Standardization: Geneva, Switzerland, 2016.
22. Hassan, A.A.; Rakha, H.A. A fully-distributed heuristic algorithm for control of autonomous vehicle movements at isolated intersections. *Int. J. Transp. Sci. Technol.* **2014**, *3*, 297–309. [[CrossRef](#)]
23. Obregón-Biosca, S. Speed humps and speed tables: Externalities on vehicle speed, pollutant emissions and fuel consumption. *Results Eng.* **2020**, *5*, 100089. [[CrossRef](#)]
24. Todalshaug, J.H.; Ásgeirsson, G.S.; Hjálmarsson, E.; Maillet, J.; Möller, P.; Pires, P.; Guérinel, M.; Lopes, M. Tank testing of an inherently phase-controlled wave energy converter. *Int. J. Mar. Energy* **2016**, *15*, 68–84. [[CrossRef](#)]
25. Chaturvedi, D.K. *Modeling and Simulation of Systems Using MATLAB and Simulink*; CRC Press: Boca Raton, FL, USA, 2017.
26. Percival, D.B.; Walden, A.T. *Spectral Analysis for Physical Applications*; Cambridge University Press: Cambridge, UK, 1993.
27. Youngworth, R.N.; Gallagher, B.B.; Stamper, B.L. An overview of power spectral density (psd) calculations. *Opt. Manuf. Test. VI* **2005**, *5869*, 206–216.
28. Múčka, P. Simulated road profiles according to iso 8608 in vibration analysis. *J. Test. Eval.* **2017**, *46*, 405–418. [[CrossRef](#)]
29. Sayers, M.W. *Guidelines for Conducting and Calibrating Road Roughness Measurements*; Technical Report; University of Michigan, Ann Arbor, Transportation Research Institute: Ann Arbor, MI, USA, 1986.
30. Sayers, M.W. On the calculation of international roughness index from longitudinal road profile. In *Transportation Research Record*; 1995. Available online: <https://trid.trb.org/View/452992> (accessed on 5 August 2024).
31. Halvorsen, E. Energy harvesters driven by broadband random vibrations. *J. Microelectromechanical Syst.* **2008**, *17*, 1061–1071. [[CrossRef](#)]
32. Swati; Singh, U.; Dahlsten, O.C.O. Quantifying the value of transient voltage sources. *Phys. Rev. Appl.* **2022**, *18*, 054064. [[CrossRef](#)]
33. El-hami, M.; Glynne-Jones, P.; White, N.M.; Hill, M.; Beeby, S.; James, E.; Brown, A.D.; Ross, J.N. Design and fabrication of a new vibration-based electromechanical power generator. *Sens. Actuators A Phys.* **2001**, *92*, 335–342. [[CrossRef](#)]

Disclaimer/Publisher’s Note: The statements, opinions and data contained in all publications are solely those of the individual author(s) and contributor(s) and not of MDPI and/or the editor(s). MDPI and/or the editor(s) disclaim responsibility for any injury to people or property resulting from any ideas, methods, instructions or products referred to in the content.